NUCLEAR THEORY, Vol. 29 (2010)
eds. A. Georgieva, N. Minkov, Heron Press, Sofia

Fast-Timing Measurements in ^{103,105,107}Cd

S. Kisyov[1], **S. Lalkovski**[1], **N. Mărginean**[2], **D. Bucurescu**[2], **L. Atanasova**[3], **D. L. Balabanski**[3], **Gh. Cata-Danil**[2], **I. Cata-Danil**[2], **J.-M. Daugas**[4], **D. Deleanu**[2], **P. Detistov**[3], **D. Filipescu**[2], **G. Georgiev**[5], **D. Ghita**[2], **T. Glodariu**[2], **J. Jolie**[6], **D.S. Judson**[7], **R. Lozeva**[5], **R. Mărginean**[2], **C. Mihai**[2], **A. Negret**[2], **S. Pascu**[2], **D. Radulov**[1,8], **J.-M. Regis**[6], **M. Rudigier**[6], **T. Sava**[2], **L. Stroe**[2], **G. Suliman**[2], **N.V. Zamfir**[2], **M. Zhekova**[1]

[1]Faculty of Physics, University of Sofia "St. Kliment Ohridski", 1164 Sofia, Bulgaria
[2]National Institute for Physics and Nuclear Engineering "Horia Hulubei", Magurele, Romania
[3]Institute for Nuclear Research and Nuclear Energy, Bulgarian Academy of Science, 1784 Sofia, Bulgaria
[4]CEA, DAM, DIF, 91297 Arpajon, France
[5]Centre de Spectrométrie Nucleaire et Spectrometrie de Masse, 91405 Orsay-Campus, France
[6]Institut für Kernphysik, University of Cologne, Cologne, Germany
[7]Department of Physics, University of Liverpool, Liverpool, United Kingdom
[8]Katholieke Universiteit, Leuven, Belgium

Abstract. Fast-timing measurements were performed recently in the region of the medium-mass ^{103,105,107}Cd isotopes, produced in fusion evaporation reactions. Emitted γ-rays were detected by eight HPGe and five $LaBr_3$:Ce detectors working in coincidence. Results on new and re-evaluated half-lives are discussed within a systematic of transition rates. The $7/2_1^+$ states in ^{103,105,107}Cd have been interpreted as arising from a single-particle excitation. The half-life analysis of the $11/2_1^-$ states in ^{103,105,107}Cd shows no change in the collectivity of their cores.

1 Introduction

The cadmium nuclei have two protons less than Z=50 closed shell Sn isotope. Thus they are a good test case for the shell model calculations, performed for the extreme neutron-rich and neutron-deficient sides of cadmium isotopic chain [1–4]. Fingerprints of collectivity start to emerge when moving away from the shell closures towards the mid-shell, giving rise to competition between single-particle and collective degrees of freedom. Signatures of collectivity in even-even cadmium nuclei can be found in the decrease of the 2_1^+ state energy when moving away from ^{98}Cd [5]. The increase of the degree of collectivity towards

the neutron mid-shell is also supported by the increase of the B(E2;$2_1^+ \rightarrow 0_1^+$) values towards the ^{116}Cd [5].

In the odd-A cadmium nuclei, band-like structures built on $11/2^-$ states are observed [5]. They have been interpreted as collective bands, based on the $\nu h_{11/2}$ intruder state. The nucleons, placed on this intruder orbital tend to polarize the core towards larger quadruple deformation. Even though the $\nu h_{11/2}$ unique parity state, which appears above the ground state in the light odd-mass cadmium isotopes, decreases in energy towards the neutron mid-shell, it never becomes a ground state. This might be related to the fact that the even-even cadmium isotopes never develop stronger quadruple deformation in their ground state, as in the nuclei placed deeper bellow the Z=50 shell gap. However, the structure of the bands, built on the $11/2^-$ state resemble the decoupled negative-parity bands observed in the medium mass palladium nuclei, [6] for example, which is a prerequisite for the increase of quadrupole deformation with respect to the ground state.

From a single-particle point of view, the ground states $J^\pi = 5/2^+$ and the first excited states $J^\pi = 7/2^+$ of ^{103}Cd, ^{105}Cd and ^{107}Cd, can be interpreted as arrising from the $\nu d_{5/2}$ and $\nu g_{7/2}$ shell-model configurations [7–9]. From a collective point of view, however, the presence of a low-lying $J^\pi = 7/2^+$ can be interpreted as a collective excitation, built on the $\nu d_{5/2}$ ground state.

In order to study the structure of these low-lying states fast-timing measurements were performed. The half-lives measured are directly related to the transitions rates, hense to their internal structure. The present paper reports on new results, obtained with eight HPGe detectors working in coincidence with five $LaBr_3$:Ce detectors.

2 Experimental Set Up and Data Analysis

The low-lying excited states, placed on and close to the yrast line in ^{103}Cd, ^{105}Cd and ^{107}Cd were populated via fusion evaporation reactions. A carbon beam, accelerated to 50 MeV with the Tandem accelerator of the National Institute for Physics and Nuclear Engineering at Magurele, Romania, impinged on self-supporting 10 mg/cm^2 thick ^{94,96}Mo targets and on a 1 mg/cm^2 thick ^{98}Mo target with 10 μm Pb backing. The three targets were isotopically enriched up to 98.97% in ^{94}Mo, 95.70% in ^{96}Mo and 98% in ^{98}Mo, respectively.

The cross section for the ^{94}Mo(^{12}C,3n)^{103}Cd reaction was calculated to be 100 mb, while for the ^{96}Mo(^{12}C,3n)^{105}Cd and ^{98}Mo(^{12}C,3n)^{107}Cd reactions it was approximately 400 mb. The typical beam intensity was of order of 8 pnA. Besides the 3n channels, the 4n, 2np, 4np and 2nα- fusion evaporation channels also have significant cross sections which contaminate the energy and time spectra of interest.

The half-lives of the levels of interest were deduced by using a fast-timing set up consisting of 5 $LaBr_3$:Ce scintillator detectors working in coincidences with 8 HPGe detectors [11]. Five of the HPGe detectors were placed at back-

ward angles with respect to the beam axis. Two of the HPGe detectors were placed at 90° with respect to the beam axis and the eighth HPGe detector was placed at a forward angle. The five $LaBr_3$:Ce detectors were mounted bellow the target chamber on a ring of approximately 45° degrees with respect to the beam axis. Each of the five $LaBr_3$:Ce crystals was of cylindrical shape and had 5% Ce doping. One of the $LaBr_3$:Ce detector was an integral detector, commercially available from Saint Gobain crystals. Its size was 2"×2". Two of the $LaBr_3$:Ce detectors had 1" height and a diameter of 1". Two $LaBr_3$:Ce crystals had dimensions of 1.5"×1.5". Each of the four non-comercial detectors was optically coupled to XP20D0B photomultiplier and mounted in aluminum casing. The readout from each of the four non-comrcial detectors, was made via a VD184/T voltage divider delivered by Photonis. The voltage divider issues a negative anode signal and a fast positive dynode signal. The anode signal was used for timing, while the dynode signal was used to obtain energy signal. This non conventional choice was made to avoid the saturation of the dynode signal [11], which facilitates the analysis of the energy spectra.

The energy signals from the HPGe detectors were analyzed by Canberra 2022 amplifiers and digitized by 8k Analog to Digital Converters (ADC) AD413A, produced by Ortec. The timing signals from the HPGe detectors were processed by 4k 4418/T Time-to-Digital Silena converters. The energy signals from the $LaBr_3$:Ce detectors were taken from the anode output of the photomultiplier's base. They were amplified and shaped by Canberra 2026 spectroscopic amplifier and then digitized by 8k ADC AD413A, supplied by Ortec. The timing signal from the $LaBr_3$:Ce detectors, taken from the anode output of the photomultiplier's base, were sent to a Quad Constant Fraction Discriminator, model 935, from Ortec. Each of the five time signals were used to start a Time-to-Amplitude Converter (TAC) operating in a common stop mode. Then the five TAC output signals were sent to 8k Silena ADC. The γ-ray array was triggered when two $LaBr_3$:Ce and one HPGe detectors were fired in coincidences.

Data was stored in event-by-event mode in 200 Mb long files, which were taken for approximately 2 hours each. Then the data was analyzed by using the GASPWare and Radware [12] packages. The walk of the CFD as a function of energy was corrected by using the procedure used in [11]. Because of the instability of the $LaBr_3$:Ce detectors observed with time, a gain matching procedure was applied file-by-file. Then the data was sorted in three dimensional energy-energy-time matrices. The half-life of the level of interest was obtained with a two-dimensional gate on the γ-ray energies detected by two $LaBr_3$:Ce detectors fired in coincidence and projected on the time axis. The three dimensional matrices were constructed after gates imposed on HPGe detectors. They have been used to select the reaction channel and the particular γ-decay branch leading to the state of interest.

Figure 1(a) and 1(b) show the energy total projection for the $^{12}\mathrm{C} + {}^{96}\mathrm{Mo} \rightarrow {}^{105}\mathrm{Cd} + 3n$ reaction for all HPGe and $LaBr_3$:Ce detectors. At low energies, the higher efficiency of the $LaBr_3$:Ce with respect to the HPGe detectors is remark-

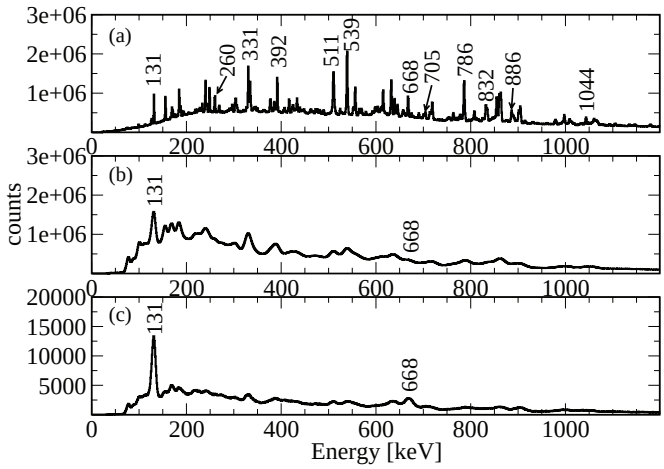

Figure 1. ^{105}Cd energy spectra: (a) Total projection with all HPGe detectors; (b) Total projection with all $LaBr_3$:Ce; (c) $LaBr_3$:Ce energy spectrum gated on 886-keV transition with any of the HPGe detectors. The labels denote known transitions in ^{105}Cd

able. The energies of ^{105}Cd are denoted with numbers. Figure 1(c) represents the $LaBr_3$:Ce energy spectrum, gated on the 886-keV transition from ^{105}Cd in the HPGe detectors, which improves the peak-to-background ratio. Similar spectra were constructed for the other two reactions $^{12}\mathrm{C} + {}^{94}\mathrm{Mo} \rightarrow {}^{103}\mathrm{Cd} + 3n$ and $^{12}\mathrm{C} + {}^{98}\mathrm{Mo} \rightarrow {}^{107}\mathrm{Cd} + 3n$. Partial level schemes, showing transitions feeding and de-exciting the $7/2^+_1$ states in ^{103,105,107}Cd, are presented in Figure 2.

Figure 3 presents time spectra obtained after two dimensional energy gates imposed on E_γ-$E_\gamma - \Delta T$ matrices, constructed for $^{103-107}$Cd. The time spectra,

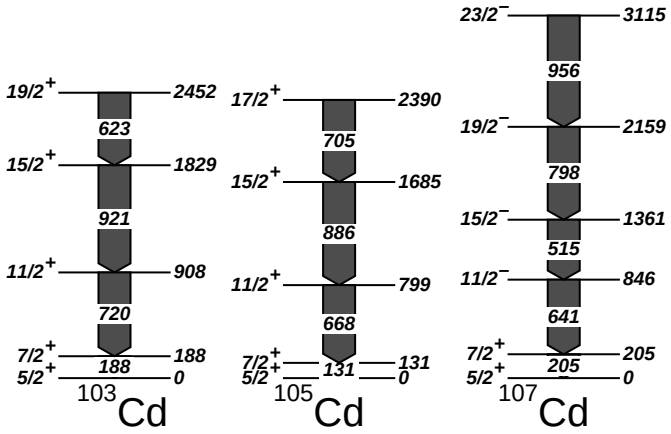

Figure 2. Partial level schemes of ^{103,105,107}Cd

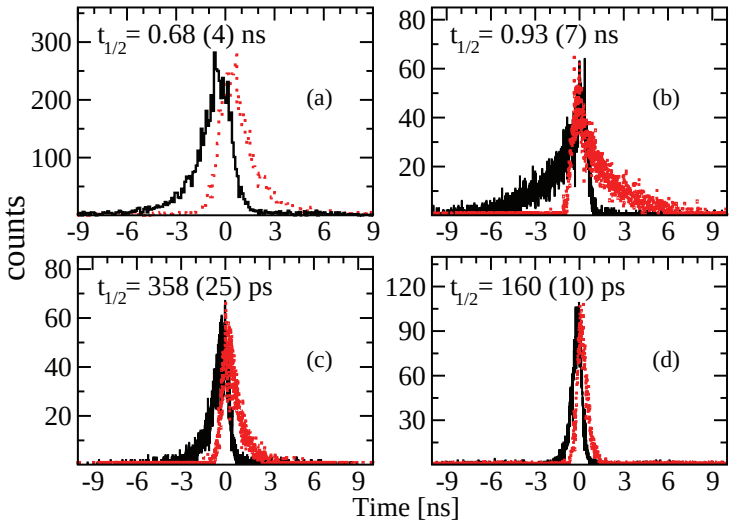

Figure 3. Time spectra, obtained for the decay of the $7/2_1^+$ states in ^{107}Cd (a), ^{105}Cd (b), ^{103}Cd (c) and for the $11/2_1^-$ state in ^{105}Cd (d)

drawn with full lines, are obtained when the feeding γ-ray with energy $E_{\gamma 1}$ is located on the x-axis of the matrix and the de-exciting transition $E_{\gamma 2}$ is located on the y-axis, i.e. the points with $(E_{\gamma 1}, E_{\gamma 2})$ coordinates on the matrix. The time spectra, drawn with dots, correspond to the opposite situation, where the feeding transition is located on y- axis, while the de-exciting transition is on x-axis, i.e. to point with $(E_{\gamma 2}, E_{\gamma 1})$ coordinates. The time, associated to the $(E_{\gamma 1}, E_{\gamma 2})$ point, was calculated as $\Delta T = T_1 - T_2$, where T_1 and T_2 are the times related to the two γ-rays, γ_1 and γ_2. The time for the $(E_{\gamma 2}, E_{\gamma 1})$ was calculated as $\Delta T = T_2 - T_1$. Then the centroids of the $(E_{\gamma 1}, E_{\gamma 2})$ and $(E_{\gamma 2}, E_{\gamma 1})$ gated time spectra appear to be shifted by 2τ, where τ is the lifetime of the level of interest [13]. This procedure represent the centroid shift method [13], which has been successfully used in the past [14] and recently applied with $LaBr_3$:Ce detectors [11, 15].

Figure 3(a) presents the time curves for the decay of the $7/2_1^+$ state in ^{107}Cd. The half-life of 0.68 (4) ns, obtained in the present work, is consistent with the NNDC value of $T_{1/2}$ =0.71 (4) ns [9]. The time spectra, shown on Figure 3(a), were obtained by gating on the 205-keV and 641-keV γ-rays detected by the $LaBr_3$:Ce detectors and 798-keV and 956-keV gates, applied on the HPGe detectors.

Figure 3(b) presents the time curves for the decay of the $7/2_1^+$ state in ^{105}Cd. The half-life of 0.93 (7) ns, obtained in the present study, was measured from the centroid shifted time spectra gated on 668γ-131γ with the $LaBr_3$:Ce detectors and gated on the 886 γ-ray or 705-keV γ-ray in any of the eight HPGe detectors. It disagrees the 1.75 (11) ns value, adopted by NNDC [8], which is based on a

$\gamma(t)$ measurement with one NaI(Tl) detector [10].

Figure 3(c) presents the time curves for the decay of the $7/2_1^+$ state in ^{103}Cd. The half-life of 358 (25) ps was obtained from the centroid shift of the two time distributions generated with gates on the 188-keV and 720-keV transitions imposed on any two of the $LaBr_3$:Ce detectors in coincidence with the 921-keV or 623-keV γ-rays detected in any of the HPGe detectors.

The half-life of the $11/2_1^-$ state in ^{105}Cd was obtained by gating on the 539-keV feeding and 392-keV de-exciting transitions, detected by any two of the five $LaBr_3$:Ce detectors. An additional gate on the 786-keV γ-ray, which is in coincidence with the 392-keV and 786-keV transitions, was imposed on any of the HPGe detectors. The time spectra are shown at Figure 3(d). The half-life, deduced from the centroid shift of the two mirror time spectra, is 160 (10) ns.

3 Discussion

$\mathbf{7/2_1^+}$: The half-lives $T_{1/2}$, of the levels of interest, are listed in Table 1 along with the level energy E_i and the spin/parity assignments J^π. In order to calculate the partial half-lives and the reduced transition probabilities the γ-ray energies E_γ, multipolarities $L\lambda$, and mixing ratios δ, adopted by NNDC [7–9], are also listed. The $J^\pi = 7/2^+$ state is the first excited state in all three isotopes and it decays via M1+E2 transition to the ground state. An upper limit of the mixing ratio $\delta \leq 0.1$ for the $7/2_1^+ \rightarrow 5/2_1^+$ transition in ^{103}Cd has been estimated by the NNDC [7]. It has been suggested that the respective transition in ^{105}Cd is of almost pure M1 nature, however a small E2 admixture is assumed [8]. For the purpose of the current discussion an upper limit of $\delta \leq$0.1 has been assumed. The mixing ratio, adopted for the M1+E2 transition in ^{107}Cd, is $\delta =$+0.25 (1) [9].

The reduced transition probabilities, given in the last column of Table 1, were calculated using the relations $B(M1)(W.u.) = 2.202 \times 10^{-5}/(E_\gamma^3 t_{1/2}^{M1}(\gamma))$ and $B(E2)(W.u.) = 9.527 \times 10^6/(E_\gamma^5 A^{4/3} t_{1/2}^{E2}(\gamma))$, where $t_{1/2}^{M1}(\gamma) = T_{1/2} \times (1 + \delta^2)$ and $t_{1/2}^{E2}(\gamma) = T_{1/2} \times (1 + \delta^2)/\delta^2$ are the partial half-lives for M1 and E2 components of the transition.

Table 1. First excited $7/2^+$ state in ^{103,105,107}Cd and decay properties

Isotope	E_i [keV]	$T_{1/2}$	E_γ [keV]	$L\lambda$	δ	$B(\lambda L)$ [W.u.]
^{103}Cd	188	358 (25) ps	188	M1	≤ 0.1	0.0092 (7)
				E2		2.34 (17)
^{105}Cd	131	0.93 (7) ns	131	M1	≤ 0.1	0.0103 (8)
				E2		5.2 (4)
^{107}Cd	205	0.68 (4) ns	205	M1	0.25 (1)	0.00331 (20)
				E2		4.2 (4)

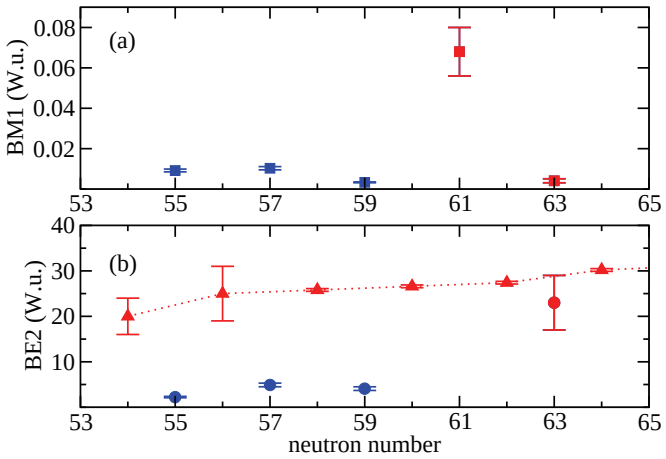

Figure 4. Systematics of B(M1;$7/2_1^+ \rightarrow 5/2_1^+$) values for odd-A cadmium isotopes (a); Systematics of B(E2;$7/2_1^+ \rightarrow 5/2_1^+$) values for odd-A cadmium isotopes (denoted with circles) compared to the B(E2;$2_1^+ \rightarrow 0_1^+$) values in even-even cadmium cores (denoted with triangles). The experimental values, obtained in the present study, are drawn in blue. The values, known prior current study, are drawn in red

Figure 4 shows the systematic trend of the B(M1) (Figure 4(a)) and B(E2) values for the $7/2_1^+ \rightarrow 5/2_1^+$ transitions in $^{103-111}$Cd (Figure 4(b)), compared to the B(E2;$2_1^+ \rightarrow 0_1^+$) for their even-even Cd cores. Figure 5 shows the evolution of the B(E2;$2_1^+ \rightarrow 0_1^+$) transition rates with the neutron number for all even-even nuclei in the $40 \leq$Z≤ 50 region.

Because of the low mixing ratio, the E2 component of the $7/2_1^+ \rightarrow 5/2_1^+$ transition is significantly hindered in the $^{103-107}$Cd nuclei comparing to their even-even Cd cores (Figure 4(b)). In fact, it is two orders of magnitude lower than the B(E2) values of the most deformed Zr and Mo nuclei, placed at the neutron-mid shell (Figure 5). In fact, the B(E2;$7/2_1^+ \rightarrow 5/2_1^+$) values, typical for the ^{103,105,107}Cd, are similar to the reduced transition probabilities for the magic tin nuclei (Figure 5) suggesting a single-particle nature of the $7/2_1^+$ state, most probably arising from $\nu g_{7/2}$ configuration.

In ^{109}Cd, the $7/2_1^+$ state appears above the first excited state with $J^\pi = 1/2^+$. Its energy is 203 keV, and decays via pure M1 transition to the ground state [16]. However, the odd behavior of the B(M1) point on Figure 4 suggests a significant E2 component.

In ^{111}Cd, the $5/2_1^+$ and $7/2_1^+$ states appear at 245 keV and 416 keV respectively [17]. The $7/2_1^+$ has a half-life of 0.12 ns and decays to the $5/2_1^+$ state via 171-keV M1+E2 transition. The mixing ratio $\delta = -0.144$ of this transition leads to B(E2;$7/2_1^+ \rightarrow 5/2_1^+$)=20.5 (2) W.u., which approaches the B(E2;$2_1^+ \rightarrow 0_1^+$) value in the even-even cadmium cores (Figure 4(b)).

$\mathbf{11/2_1^-}$: The $J^\pi = 11/2_1^-$ states appear in all odd-cadmium isotopes from

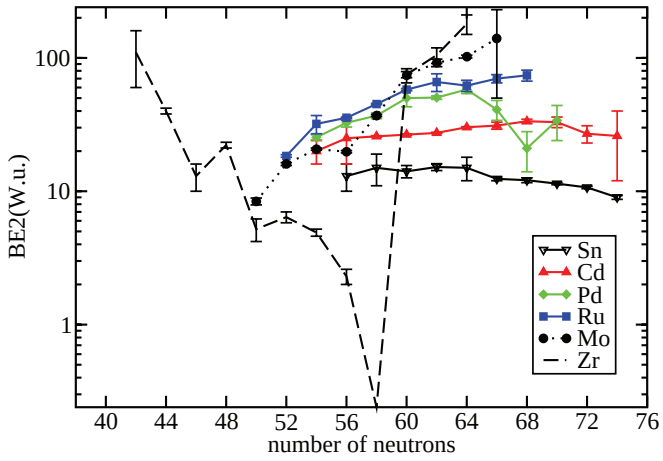

Figure 5. Systematics of B(E2;$2_1^+ \rightarrow 0_1^+$) transition rates for the even-even nuclei with $40 \leq Z \leq 50$

^{103}Cd to ^{123}Cd [5]. It is observed at 1671 keV in ^{103}Cd [7] and decreases in energy when approaching the neutron mid-shell. In ^{117}Cd$_{69}$ it appears at 136 keV above the ground state.

The big energy gap between the $11/2_1^-$ state and the ground state in $^{103-111}$Cd opens space for several states of single-particle and collective nature to appear. Among those states is the $9/2_1^+$ state to which the $11/2_1^-$ state decays via an E1 transition. For medium mass odd-A Cd isotopes the energy of the $11/2_1^-$ drops closer to the ground state where only low-spin states are populated. In this mass region the $11/2_1^-$ state decays via low-energy transitions of higher multipolarity leading to increase of its half-life to $T_{1/2}$ =14.1 y in ^{113}Cd [5]. Further increases of the energy of the $11/2_1^-$ state with respect to the ground state leads to a decrease of the half-life. The isomeric $11/2_1^-$ state in all neutron-rich cadmium nuclei with A$\geq$113 decay via β-decay process to the respective indium isobars. In spite the half-life of the state decreases and the energy of the isomeric state increases with the mass number, isomeric decays have not been observed so far.

The half-life of the excited $11/2_1^-$ state in ^{103,105}Cd, measured in present work, allows a systematical study of the E1 transitions. The half-life $T_{1/2}$=71 ns of the $11/2_1^-$ state in ^{107}Cd has been measured [10]. This level decays via a branch of E1, M2 and E3 transitions to $9/2^+$, $7/2^+$ and $5/2^+$ states with partial half-lives 2.4×10^{-7}, 1.0×10^{-7} and 4.5×10^{-6} s respectively.

The $11/2_1^-$ state in ^{105}Cd decays via two E1 transitions to two $9/2^+$ states. The partial half-lives for the two transitions are 3.1×10^{-10} and 3.7×10^{-10} s respectively.

The $11/2^-$ state in ^{103}Cd decays via 931-keV E1 transition. No time structure of the decaying transition has been observed in the present work. Therefore, an upper limit of 6 ps has been deduced.

The Weisskopf estimates for the 931-keV E1 γ-ray in ^{103}Cd is $T_{1/2}^{W.e.} = 3.8 \times 10^{-16}$ s, for the 330-keV E1 transition and 392-keV E1 γ-ray in ^{105}Cd are 8.40×10^{-15} s and 5.00×10^{-15} s. and $T_{1/2}^{W.e.} = 6.14 \times 10^{-12}$ s for the 37-keV E1 transition in ^{107}Cd. For all four transitions the E1 hindrance factor $F^W = T_{1/2,\gamma}/T_{1/2}^{W.e.}$ is of order of 10^4 which suggests a similar collective structure of the $11/2_1^-$ state for the three cadmium isotopes with A=103,105,107.

4 Conclusion

Excited states in ^{103,105,107}Cd have been populated via fusion-evaporation reactions. Half-lives of several excited states were measured by using the delayed coincidence technique. The half-life of the $7/2_1^+$ state in ^{107}Cd has been confirmed. The half-life of the $7/2_1^+$ state in ^{105}Cd is re-evaluated. The half-life of the first excited state in ^{103}Cd and of the $11/2_1^-$ in ^{105}Cd are newly obtained. Reduced transition probabilities have been calculated for several excited states. The E2 component of the $7/2_1^+ \rightarrow 5/2_1^+$ transitions are strongly hindered with respect to the B(E2) transitions, observed in the most deformed nuclei in the region suggesting a single particle nature for the $7/2_1^+$ states. The hindrance factors, calculated from the experimental half-lives of the $11/2_1^-$ states in ^{103,105,107}Cd, are of same order of magnitude suggesting similar collectivity in all three nuclei.

Acknowledgments

The work is partly supported by the Bulgarian Science Fund under contract numbers DMU02/1, DRNF02/5, DID-05/16 and by a contract for Bularian-Romanian partnership, number BRS-07/23.

References

[1] A. Jungclaus *et al.*, *Phys. Rev. Lett.* **99** (2007) 132501.
[2] L. Caceres *et al.*, *Phys. Rev. C* **79** (2009) 011301.
[3] F. Naqvi *et al.*, *Phys. Rev. C* **82** (2010) 034323.
[4] A. Blazhev *et al.*, *Phys. Rev. C* **69** (2004) 064304
[5] NNDC data base (www.nndc.bnl.gov).
[6] D. Kutsarova *et al.*, *Phys. Rev. C* **58** (1998) 1966.
[7] D. de Frenne, *Nucl. Data Sheets* **110** (2009) 2081
[8] D. de Frenne and E. Jacobs, *Nucl. Data Sheets* **105** (2005) 775.
[9] J. Blachot, *Nucl. Data Sheets* **109** (2008) 1383.
[10] R. Rougny, M. Meyer-Lévy, R. Béraud, J Rivier and R. Moret, *Phys. Rev. C* **8** (1973) 2332.
[11] N. Marginean *et al.*, *Eur. Phys. J. A* (accepted).
[12] D. Radford, *Nucl. Instr. Meth.* **A361** (1995) 297.
[13] W. Andrejtscheff, M. Senba, N. Tsoupas and Z. Z. Ding, *Nucl. Instr. Meth.* **204** (1982) 123.

[14] W. Andrejtscheff, L. K. Kostov, H. Rotter, H. Prade, F. Stary, M. Senba, N. Tsoupas, Z. Z. Ding and P. Raghavan, *Nucl. Phys.* **A437** (1985) 167.
[15] J.-M. Regis, G. Pascovici, J. Jolie, M. Rudigier, *Nucl. Instr. Meth.* **A622** (2010) 83.
[16] J. Blachot, *Nucl. Data Sheets* **107** (2006) 355.
[17] J. Blachot, *Nucl. Data Sheets* **110** (2009) 1239.